The Journal of Neuroscience, December 1, 1998, *18*(23):9638–9649

A Product of the *Drosophila stoned* Locus Regulates Neurotransmitter Release

Daniel T. Stimson,[1] Patricia S. Estes,[1] Michiko Smith,[2] Leonard E. Kelly,[2] and Mani Ramaswami[1]

[1]Arizona Research Laboratories Division of Neurobiology and Department of Molecular and Cellular Biology, University of Arizona, Tucson, Arizona 85721, and [2]Department of Genetics, University of Melbourne, Parkville, Australia

The *Drosophila stoned* locus encodes two novel gene products termed stonedA and stonedB, which possess sequence motifs shared by proteins involved in intracellular vesicle traffic. A specific requirement for *stoned* in the synaptic vesicle cycle has been suggested by synthetic genetic interactions between *stoned* and *shibire*, a gene essential for synaptic vesicle recycling (Petrovich et al., 1993). A synaptic role of *stoned* gene products also is suggested by altered synaptic transients in electroretinograms recorded from *stoned* mutant eyes (Petrovich et al., 1993). We show here that the stonedA protein is highly enriched at *Drosophila* nerve terminals. Mutant alleles that affect stonedA disrupt the normal regulation of synaptic vesicle exocytosis at neuromuscular synapses of *Drosophila*. Spontaneous neurotransmitter release is enhanced dramatically, and evoked release is reduced substantially in such *stoned* mutants. Ultrastructural studies reveal no evidence of major disorganization at *stoned* mutant nerve terminals. Thus, our data indicate a direct role for stonedA in regulating synaptic vesicle exocytosis. However, genetic and morphological observations suggest additional, subtle effects of *stoned* mutations on synaptic vesicle recycling. Remarkably, almost all phenotypes of *stoned* mutants are similar to those previously described for mutants of synaptotagmin, a protein postulated to regulate both exocytosis and the recycling of synaptic vesicles. We propose a model in which stonedA functions together with synaptotagmin to regulate synaptic vesicle cycling.

Key words: neurogenetics; stoned; Drosophila; *presynaptic function; neurotransmitter release; synaptic vesicle fusion; synaptic vesicle recycling*

Chemical synaptic transmission requires the release of neurotransmitter via the fusion of transmitter-filled synaptic vesicles to the presynaptic plasma membrane (for review, see Sudhof, 1995; Matthews, 1996). Although spontaneous synaptic vesicle fusions occur at a low rate in the absence of extracellular Ca^{2+} (Katz, 1969), stimulus-evoked vesicle fusion depends on the influx of extracellular Ca^{2+} into the presynaptic terminal (Zucker, 1996). Ca^{2+} is known to trigger synaptic vesicle fusion by altering dynamic interactions between vesicle-associated proteins and plasma membrane-associated proteins (Sudhof, 1995; Hanson et al., 1997). The synaptic vesicle protein synaptotagmin is believed to act as a Ca^{2+} sensor that not only inhibits spontaneous Ca^{2+}-independent vesicle fusion but also promotes Ca^{2+}-evoked exocytosis (DiAntonio et al., 1993; Littleton et al., 1993, 1994; DiAntonio and Schwarz, 1994; Geppert et al., 1994; Sudhof and Rizo, 1996).

Subsequent to fusion, synaptic vesicle proteins deposited in plasma membrane are retrieved by endocytosis and recycled into new synaptic vesicles (Kelly, 1993; Cremona and De Camilli, 1997). The budding of endocytic vesicles from presynaptic membrane appears to involve clathrin and several associated proteins, including the adaptor complex AP-2 (De Camilli and Takei, 1996; Robinson, 1997). Fission of budding vesicles from the plasma membrane occurs by a mechanism requiring the GTPase dynamin, which is altered in *Drosophila shibire* (shi^{ts}) mutants that show a conditional block in synaptic vesicle endocytosis (Kosaka and Ikeda, 1983; van der Bliek and Meyerowitz, 1991; De Camilli and Takei, 1996; Warnock and Schmid, 1996; Grant et al., 1998). Despite this emerging outline of molecular mechanisms that underlie synaptic vesicle cycling (for review, see Cremona and De Camilli, 1997), it is likely that several molecules that participate in the process remain to be identified and studied.

Classical genetic studies provide one avenue for the characterization of such gene products. Previous studies of *Drosophila stoned* mutants have suggested that *stoned* (*stn*) gene products serve important neuronal functions. The mutants stn^{ts2} and stn^{c} exhibit behavioral defects; most notably they are sluggish and uncoordinated, suggesting defects of nervous system function (Petrovich et al., 1993). Transients of the electroretinogram, which are believed to represent synaptic transmission between the photoreceptor layer and the lamina within the fly visual system, are altered in stn^{ts2} (Kelly, 1983) and in stn^{c} mutants (Homyk and Pye, 1989), suggesting defects in synapse development or function. Genetic interactions between *stoned* and *shibire* mutations may indicate a more specific neuronal function for *stoned*. The

Received June 29, 1998; revised Sept. 3, 1998; accepted Sept. 10, 1998.

This work was funded by National Institutes of Health Grant NS34889 (to M.R.) as well as by the McKnight and Alfred P. Sloan foundations. D.S. acknowledges support from Developmental Neuroscience Research Training Grants at the University of Arizona, funded by the Flinn Foundation and National Institutes of Health. We thank A. Marie Phillips for permission to cite her unpublished results and K. S. Krishnan, Sujata Rao, and A. Marie Phillips for useful discussions. We are grateful to Rick Levine and Andrea Yool as well as to Christos Consoulas and Rebecca Johnston of the Levine lab for help with electrophysiology. We acknowledge Patty Jansma for assistance with confocal and electron microscopy. We also thank John Calley for his help in searching protein databases. The microscopy was performed with a Bio-Rad 600 confocal microscope and a Jeol 200EX electron microscope belonging to the Arizona Research Laboratories Division of Neurobiology. We thank Troy Littleton and Hugo Bellen for anti-syt antibodies and Erich Buchner and Konrad Zinsmaier for anti-csp antibodies. This manuscript was improved substantially by comments from Rick Levine and Dave Sandstrom.

Correspondence should be addressed to Daniel T. Stimson, Department of Molecular and Cellular Biology, Life Sciences South, Room 444, University of Arizona, P.O. Box 210106, Tucson, AZ 85721.

stn^{ts2} mutation produces synthetic lethality when combined with *shi*^{ts1}, suggesting a possible role for *stoned* gene products in synaptic vesicle recycling (Petrovich et al., 1993).

Such a role for *stoned* in endocytosis is indicated further by a detailed analysis of the sequence of *stoned* (Andrews et al., 1996) (see Fig. 7). The *stoned* gene gives rise to a dicistronic mRNA that encodes two structurally unrelated proteins, stonedA and stonedB, from separate open reading frames (ORFs) (Andrews et al., 1996). Both proteins possess sequence motifs found in proteins known or suspected to regulate endocytic vesicle traffic (see Fig. 7). StonedB contains a C-terminal region with 42% identity to a family of adaptor subunit proteins (Andrews et al., 1996) and an N-terminal region with seven repeats of the trimer NPF, recently identified as a consensus binding motif for the clathrin and adaptor-associated protein Eps15 (Benmerah et al., 1996; Salcini et al., 1997). More sequence analysis presented here (see Fig. 7) shows that stonedA also contains sequence motifs characteristic of molecules involved in endocytosis. Taken together with the genetic interaction between *stn*^{ts2} and *shi*^{ts1}, the structural features of stonedA and stonedB suggest that both proteins have presynaptic functions, possibly in clathrin-mediated endocytosis (Andrews et al., 1996; Cremona and De Camilli, 1997).

To investigate directly the potential synaptic functions of the *stoned* gene products, we examined the effects of *stoned* mutations on the function and morphology of synapses on muscles 6 and 7 of the *Drosophila* third instar larval body wall (Jan and Jan, 1976; Atwood et al., 1993; Kurdyak et al., 1994). Via combined physiological and morphological analyses of *stn*^{ts2} and *stn*^{c} synapses, we show that *stoned* mutations appear to have direct effects on the regulation of neurotransmitter release. Our results also suggest additional subtle effects of *stoned* mutations on synaptic vesicle recycling and synapse plasticity. During the course of this study it was discovered that *stn*^{ts2} and *stn*^{c} both carry missense mutations within the first ORF of *stoned*, causing single amino acid substitutions within stonedA (A. M. Phillips and M. Smith, unpublished observations). Thus, our phenotypic characterization of *stn*^{ts2} and *stn*^{c} mutants provides direct evidence that a *stoned* gene product, specifically stonedA, acts as a novel regulator of neurotransmitter release.

MATERIALS AND METHODS

Drosophila *culture.* Flies were raised in vials on instant fly food (Carolina Biological Supply, Burlington, NC) or on medium consisting of instant fly food, agar, and oatmeal (Condie and Brower, 1989) supplemented with yeast. All stocks were maintained at 20–21°C under uncrowded conditions.

Drosophila *strains and genetics.* Two different wild-type *Oregon-R* stocks were used, one deriving from Seymour Benzer's lab (Caltech, Pasadena, CA) and one from Danny Brower's lab (University of Arizona, Tucson, AZ). *stoned* mutants *stn*^{ts2}, *stn*^{c}, *stn*$^{13–120}$, and *stn*^{PH1} were from Len Kelly's (University of Melbourne, Parkville, Australia) laboratory. The *stoned* lethal alleles *stn*$^{13–120}$ and *stn*^{PH1} are caused by transposon insertions within the stonedA and stonedB ORFs, respectively (Andrews et al., 1996). Whereas *stn*$^{13–120}$ was isolated in a wild-type background, the *stn*^{PH1} allele was isolated on a complex chromosome carrying multiple inversions (Zusman et al., 1985); this complex background may cause phenotypes unlinked to *stoned*. The failure of *stn*$^{13–120}$ and *stn*^{PH1} to complement each other suggests that each may impair translation of both stonedA and stonedB proteins via a combination of mRNA truncation and/or polarity effects (Andrews et al., 1996).

To map *stn*^{ts2} and *stn*^{c} physiological phenotypes to the *stoned* locus, we first mapped these phenotypes to the X chromosome by setting up reciprocal crosses between *Oregon-R* and *stn*^{ts2} or *stn*^{c}. Subsequently, we ascertained that the *stoned* phenotypes were rescued by a duplication of *stoned* and uncovered by *stn*$^{13–120}$ and *stn*^{PH1} as well as a deficiency for *stoned*. The duplication *Dp(1,Y) y*$^{+}$*Ymal*$^{+}$, which consists of a proximal piece of the X chromosome including *stoned* attached to the Y chromosome, was from Len Kelly's laboratory or from the Tata Institute of Fundamental Research, Bombay stock collection. The deficiency stock *Df(1)HM430*, which covers X chromosome region 20 between *uncl* and *l(1)20Cb*, was a generous gift of Maurice Kernan (State University of New York, Stony Brook, NY). *Df(1)HM430*, *stn*$^{13–120}$, and *stn*^{PH1} were maintained in stocks over balancers (e.g., *FM6*) or over *y*$^{+}$*Ymal*$^{+}$. Because *Df(1)HM430* and *stn*$^{13–120}$ could be maintained over *y*$^{+}$*Ymal*$^{+}$, flies of the genotypes *stn*^{c}/*stn*$^{13–120}$, *stn*^{ts2}/*stn*$^{13–120}$, *stn*^{c}/*Df(stn)*, *stn*^{ts2}/*Df(stn)*, *stn*^{c}/*y*$^{+}$*Ymal*$^{+}$, and *stn*^{ts2}/*y*$^{+}$*Ymal*$^{+}$ could be generated easily from crosses similar to those shown below:

$$stn^{13\text{-}120}/y^{+}Ymal^{+} \times stn^{ts2}/stn^{ts2}$$
$$\downarrow$$
$$stn^{ts2}/stn^{13\text{-}120} + stn^{ts2}/y^{+}Ymal^{+}$$
$$\text{OR}$$
$$Df(1)HM430/y^{+}Ymal^{+} \times stn^{ts2}/stn^{ts2}$$
$$\downarrow$$
$$stn^{ts2}/Df(1)HM430 + stn^{ts2}/y^{+}Ymal^{+}.$$

We controlled extensively for genetic background effects. In larvae of the genotype *stoned*^{viable}/*y*$^{+}$*Ymal*$^{+}$, the duplication was derived from one of two different parental stocks (*stn*$^{13–120}$/*y*$^{+}$*Ymal*$^{+}$ or *Df(1)HM430*/*y*$^{+}$*Ymal*$^{+}$). Regardless of parental origin, *y*$^{+}$*Ymal*$^{+}$ always complemented *stoned*^{viable} phenotypes, except where noted in the text. *stn*^{PH1}/*y*$^{+}$*Ymal*$^{+}$ males were usually inviable and, in our hands, survivors were typically sterile. Therefore, *stn*^{PH1} was maintained over *FM6(T8-lacz)*, which drives the expression of β-galactosidase from the *asense* promoter. Female progeny from the cross *stoned*^{viable}/*Y* × *stn*^{PH1}/*FM6(T8-lacz)* were selected for electrophysiology and subsequently were processed for β-galactosidase activity to score the genotype. Briefly, larval CNSs were dissected away and fixed for 3 min in 3% glutaraldehyde in PBS. Fixed CNSs were incubated for 2.5 hr at 37°C in staining solution containing (in mM) 10 PO_4 buffer, pH 7.2, 150 NaCl, 1 $MgCl_2$, 3 $K_4[FeII(Cn)_6]$, and 3 $K_3[FeIII(Cn)_6]$ plus 0.2% Triton X-100. Just before incubation, a 1:50 volume of freshly prepared 10% X-gal in DMSO was added to staining solution that had been preheated to 65°C. The absence of characteristic blue staining within the CNS was used to identify larvae of the genotype *stoned*^{viable}/*stn*^{PH1}.

Larval neuromuscular preparations. For electrophysiology and microscopy of larval neuromuscular junctions (NMJs), larvae were selected from the stocks and dissected to expose the larval body wall muscles, as described previously (Estes et al., 1996). All experiments were performed on muscles 6 and 7 within the third abdominal segment (A3), with the exception of electron microscopy (EM) and stonedA immunohistochemistry studies, in which A2 was included. Muscles 6 and 7 are innervated by a pair of identified motor neurons with well characterized physiological and morphological properties (Jan and Jan, 1976; Atwood et al., 1993; Kurdyak et al., 1994). The motor neurons have distinct firing thresholds and generate a compound response in muscle when they fire simultaneously. During dissections and electrophysiological experiments the larvae were immersed in "HL3" saline (Stewart et al., 1994), which contains (in mM) 70 NaCl, 5 KCl, 1.5 $CaCl_2$, 20 $MgCl_2$, 10 $NaHCO_3$, 5 trehalose, 115 sucrose, and 5 HEPES, pH 7.3. Of those available, the HL3 saline recipe produces an ionic composition and osmolarity most similar to that of *Drosophila* hemolymph (Stewart et al., 1994). To prevent muscle contraction that potentially could damage the preparation during dissection, we dissected larvae in low Ca^{2+} saline or in Ca^{2+}-free saline in which the $CaCl_2$ was replaced by 1.5 mM $MgCl_2$ and 0.5 mM EGTA. These treatments did not have any distinguishable effects on the electrophysiological properties of the NMJ.

Electrophysiology. All electrophysiological recordings were made from muscle 6, with the larval preparation immersed in a low volume of the HL3 saline described above. Temperature of the saline was 19–21°C, and was checked often with a thermocouple microprobe (type IT-21, Physitemp, Clifton, NJ). Where noted in the text, Ca^{2+} concentration sometimes was reduced to subphysiological levels by replacing $CaCl_2$ with $MgCl_2$. In all preparations the CNS was gently cut away to prevent endogenous motor activity. Motor nerves were stimulated with glass-tipped suction electrodes. For recordings of excitatory junctional potentials (EJPs) and excitatory junctional currents (EJCs), an isolated pulse stimulator (A-M Systems, Everett, WA) was used to deliver 1 msec pulses at a frequency of 1 Hz and at an intensity ~1.5× that required to elicit the compound response. All recordings were acquired with an Axoclamp 2B amplifier in conjunction with pClamp 6 software (Axon Instruments, Foster City, CA). Recording electrodes were pulled from thick-walled

borosilicate capillary tubes (FHC, Bowdoinham, ME) with a Sutter Instruments (Novato, CA) electrode puller. For intracellular recordings the electrodes were backfilled with 2 M KAc, yielding resistances of 25–40 MΩ. For two-electrode voltage clamp (TEVC) experiments, the recording electrode was backfilled with 3 M KCl; the tip of the current-passing electrode was filled with 2 M K-citrate and the remainder was backfilled with 3 M KCl. Resistances of recording and current-passing electrodes were 10–20 and 15–35 MΩ, respectively. After impalement with both electrodes, the resting membrane potential of muscle 6 was usually at approximately −50 mV but always was clamped to −70 mV. Input resistance was determined by delivering a 20 mV hyperpolarizing pulse from the −70 mV holding potential. The EJC or EJP amplitude for each preparation was determined from an average of 10 consecutive evoked responses. During TEVC, clamp conditions were optimized so that deviation from the holding potential on stimulation was <5 mV. EJCs were low-pass-filtered at 1 kHz. Although the frequencies of mejcs and mejps appeared similar, mejp recordings were much cleaner and therefore were used to quantify mini frequencies. For each preparation, the number of mejps occurring consecutively within 10 sec was used to determine mini frequency. Although the reported mini frequencies were recorded in physiological saline (Ca^{2+} = 1.5 mM), reducing extracellular Ca^{2+} concentration did not appear to affect mini frequency significantly (data not shown).

Confocal microscopy. Dissected larvae (see above) were processed by previously described immunohistochemical procedures (Estes et al., 1996). Briefly, each was fixed in 3.5% paraformaldehyde prepared in PBS containing 0.5 mM EGTA and 0.2 mM $MgCl_2$. After washes in PBS the larval preparation was blocked in 2% BSA and 5% goat serum in PBS containing 0.15% Triton X-100 (TBS). Then the preparation was incubated for 2 hr in primary antibody at an appropriate dilution (see below), followed by a 1 hr incubation in fluorescent secondary antibody at a final dilution of 1:200. The preparation was mounted in 0.1% paraphenylene diamine (Sigma, St. Louis, MO) in 95% glycerol and viewed. Rabbit anti-synaptotagmin (DSYT-2) antibody was a generous gift from Troy Littleton and Hugo Bellen (Baylor College of Medicine, Waco, TX) and was used at a final dilution of 1:200. Mouse anti-cysteine string protein (anti-csp) antibody (mAb49), kindly provided by Erich Buchner (Universitat Wurzburg, Germany) and Konrad Zinsmaier (University of Pennsylvania School of Medicine, Philadelphia, PA), was used at a final dilution of 1:50. Rabbit anti-stonedA antiserum was generated against a stonedA–maltose binding protein (MBP) fusion protein and was used at a final dilution of 1:1000. A Texas Red-conjugated goat anti-rabbit antibody (ICN, Costa Mesa, CA) was used to visualize synaptotagmin and stonedA, and an FITC-conjugated goat anti-mouse antibody (ICN) was used to visualize csp. A Bio-Rad 600 laser-scanning confocal microscope and COMOS software (Bio-Rad, Richmond, CA) were used for all image analyses. For synaptotagmin and stonedA single-label experiments, the YHS filter supplied by Bio-Rad was used. For synaptotagmin/csp double-label experiments, the K1/K2 filter was used. For examination of bouton morphology, 1 μm optical sections were collected with the use of a 60× objective. For examination of synaptotagmin and csp distribution within boutons, 1 μm sections were collected by using 60× power at 5× zoom. Images of anti-stonedA staining were taken at 60× power, 1× zoom.

Electron microscopy. Each larval preparation was processed as described previously (Estes et al., 1996). Briefly, the dissected larva was incubated in Trump's fixative overnight at 4°C. Then the preparation was washed in 100 mM cacodylate buffer containing 264 mM sucrose. The preparation was post-fixed with 1% OsO_4 in 100 mM cacodylate buffer for 2 hr, dehydrated in an ethanol series, and embedded in Epon/Araldite (Embed 812, Electron Microscopy Sciences, Fort Washington, PA). Grids were poststained with 2% uranyl acetate and 1% lead citrate and examined under a Jeol 1200EX electron microscope. Only type I boutons on muscle 6 or 7 within A2 and A3 were selected for analysis. Synaptic vesicle content was determined by manual measurements from only those bouton cross sections that contained one or more active zones and in which subsynaptic reticulum was evident.

Statistics. Numerical data reported in the text are mean ± SEM; p values reported in the text were determined by Student's t test.

RESULTS

StonedA immunoreactivity is present at presynaptic terminals and is reduced in *stn*^{c} mutants

Given the genetic and molecular evidence that stonedA may be involved in synaptic functions, we sought evidence for the presence of stonedA at *Drosophila* synapses. Using an anti-stonedA antiserum (raised against an MBP fusion to residues 27–350 of stonedA), we observed strong immunoreactivity within motor terminals of wild-type larvae (Fig. 1). The staining was eliminated completely by the preincubation of the antiserum with a stonedA–GST fusion protein, indicating that the antiserum recognizes an epitope present on stonedA (data not shown). StonedA immunoreactivity within boutons is not attributable to cross-reacting epitopes, because it is altered substantially in *stoned* mutants. Although stonedA immunoreactivity is at nearly wild-type levels in *stn*^{ts2} boutons, it is barely detectable in *stn*^{c} mutant motor terminals (Fig. 1). The altered stonedA immunoreactivity within *stn*^{c} boutons probably indicates a reduction of stonedA protein levels at nerve terminals, rather than an altered epitope, because the presumptive *stn*^{c} mutation lies considerably C-terminal to the region of stonedA used to raise the antiserum. Most importantly, the presence of stonedA at nerve terminals suggests a presynaptic function for the protein.

In addition to stonedA immunoreactivity at presynaptic boutons, we also observed a characteristic striated pattern of staining in body wall muscle. Although this could be competed out by preincubation of the serum with stonedA fusion protein, the muscle staining was not affected significantly by the *stn*^{c} mutation. Thus, we are unable to determine whether stonedA immunoreactivity in muscles truly represents muscle expression (and potential function) of stonedA, or a conserved epitope in a different protein. However, our data unambiguously show that stonedA protein is concentrated at motor nerve terminals.

stoned mutations alter mejp frequency and EJP amplitude

To investigate the role of stonedA in synaptic transmission, we used electrophysiology to assess synaptic function at *stn*^{ts2} and *stn*^{c} mutant NMJs compared with wild-type controls. From current-clamp recordings of miniature excitatory junctional potentials (mejps) as well as TEVC recordings of currents (mejcs), we found an approximately threefold enhancement in the frequency of spontaneous miniature events (minis) at *stn*^{ts2} and *stn*^{c} NMJs relative to wild-type NMJs (Fig. 2*A*, Table 1). Mini frequencies were 4.8 ± 0.4/sec in wild-type, 14.1 ± 0.6/sec in *stn*^{ts2} ($p = 1.5 \times 10^{-11}$), and 14.2 ± 0.8/sec in *stn*^{c} ($p = 2.6 \times 10^{-8}$). The elevated mini frequency of *stn*^{ts2} and *stn*^{c} mutants indicates a relatively high rate of spontaneous synaptic vesicle fusion events at *stn*^{ts2} and *stn*^{c} motor terminals. This phenotype could result from weakened regulation of synaptic vesicle exocytosis.

In addition to altered spontaneous synaptic activity, postsynaptic responses evoked by motor nerve stimulation were altered substantially in *stn*^{c}, but not *stn*^{ts2}, mutants (Fig. 2*B*, Table 2). In physiological saline (Ca^{2+} = 1.5 mM), the peak amplitudes of EJPs in wild-type (39.2 ± 2.4 mV) and *stn*^{ts2} (41.2 ± 2.1 mV) were similar, whereas *stn*^{c} EJPs were much smaller (20.1 ± 2.4 mV) than wild-type ($p = 3.5 \times 10^{-6}$). To monitor directly the response of the muscle to neurotransmitter secretion, we eliminated voltage-activated components of the evoked response as well as nonlinear summation of quantal events by clamping wild-type and *stn*^{c} muscle fibers at −70 mV and recording the EJCs. EJC measurements revealed the true extent of defects in *stn*^{c}-evoked responses: the EJC amplitude of *stn*^{c} (17.4 ± 3.6 nA) was only 15% of that of wild-type (132.3 ± 13.8 nA; $p = 5.7 \times 10^{-5}$)

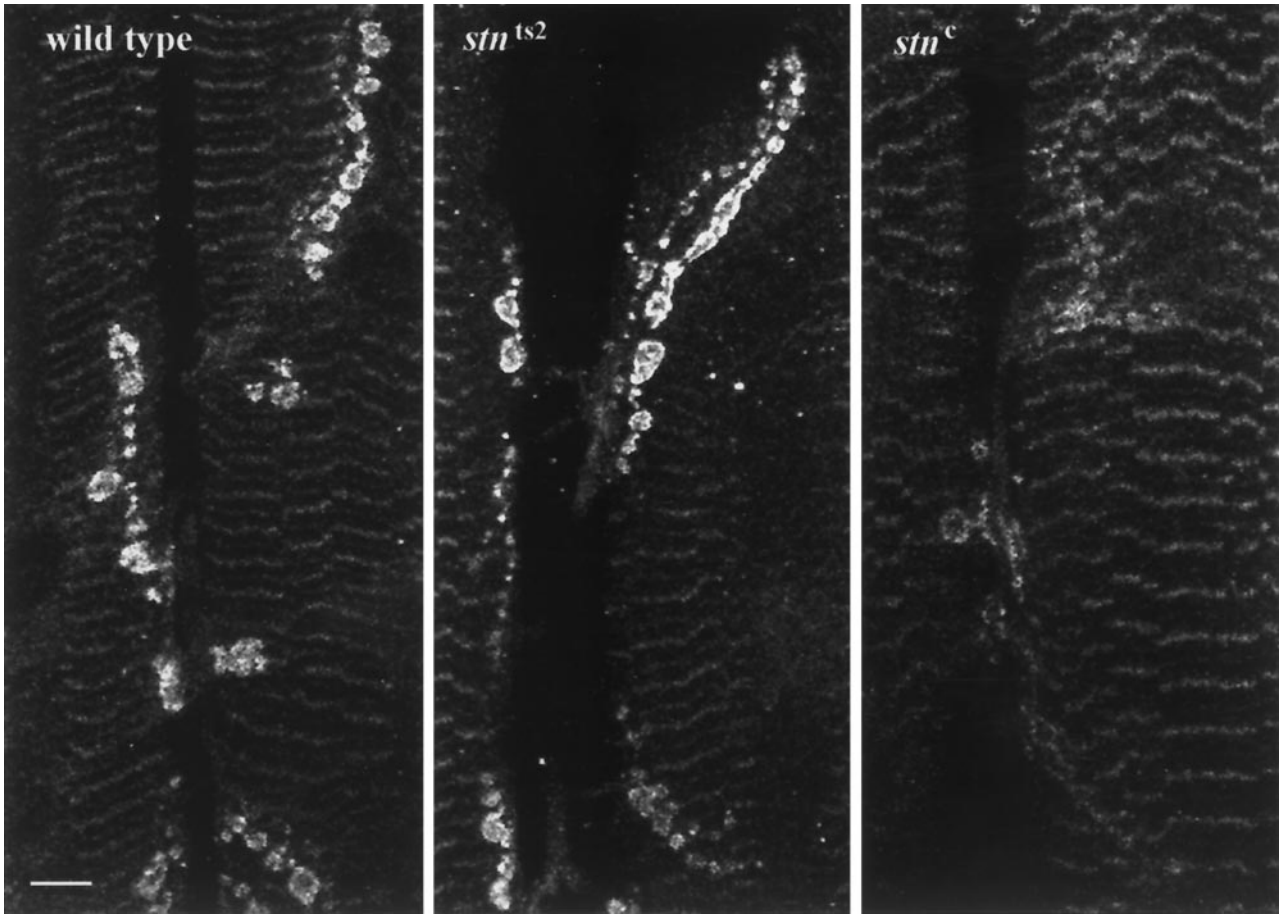

Figure 1. StonedA is highly enriched in motor terminals. In third instar larval neuromuscular synapses stained with anti-stonedA antiserum, a strong signal within wild-type and *stn* ^{ts2} presynaptic boutons is reduced significantly in *stn* ^{c}. In some *stn* ^{ts2} preparations there appeared to be a moderate reduction in stonedA immunoreactivity, but this was not seen consistently. Note that a distinct muscle staining visible in these images is not altered in *stn* ^{c} mutants. Confocal projections show representative synaptic arbors from abdominal segment A2 for each genotype. Scale bar, 10 μm. All three images were acquired with identical confocal settings. Synaptic arbors from 18 wild-type, 7 *stn* ^{ts2}, and 8 *stn* ^{c} larvae were examined.

(Fig. 2*B*). Because input resistances of *stn* ^{c} and wild-type muscles were comparable (wild-type, 3.9 ± 0.5 MΩ; *stn* ^{c}, 5.1 ± 0.75 MΩ), this difference clearly arises from defective synaptic transmission at *stn* ^{c} NMJs rather than more general defects in *stn* ^{c} muscles. The *stn* ^{ts2} allele appeared almost wild-type in EJC amplitude, suggesting that the *stn* ^{ts2} mutation affects a domain of stonedA more essential for regulating spontaneous, rather than evoked, synaptic transmission. At room temperature and in the EJC assay, *stn* ^{ts2} behaves like a weak allele of *stoned*. This is consistent with our observation that stonedA immunoreactivity is clearly reduced in *stn* ^{c}, but not *stn* ^{ts2}, mutants. Although originally isolated in a screen for mutants paralyzed at 29°C, in reality the behavioral phenotype of *stn* ^{ts2} mutants (sluggishness and uncoordination) shows minimal temperature sensitivity. Consistent with observations on the behavior of *stn* ^{ts2} mutants, there is little effect of elevated temperature (30°C) on the electrophysiological phenotypes we observe (data not shown). In summary, our physiological analysis indicates that *stoned* mutations not only elevate the frequency of spontaneous synaptic vesicle fusions but also decrease evoked synaptic transmission, phenotypes consistent with a role for stonedA in the regulation of neurotransmitter release.

We confirmed that the electrophysiological defects in *stn* ^{ts2} and *stn* ^{c} larvae derive from mutations in the *stoned* locus by ensuring that these phenotypes were uncovered by lethal genetic lesions of *stoned* and were complemented by duplications of *stoned*. For uncovering *stoned* phenotypes, we used the deficiency *Df(1)HM430*, which deletes the region of the X chromosome containing *stoned* (region 20B) and two homozygous lethal alleles of *stoned, stn* $^{13–120}$ and *stn* ^{PH1}. The duplication *Dp(1,Y) y* $^{+}$*Ymal* $^{+}$ is a modified Y chromosome carrying region 20 of the X chromosome, which includes the *stoned* locus; for simplicity, we refer to this duplication as *y* $^{+}$*Ymal* $^{+}$. As shown in Table 1, the electrophysiological phenotypes of *stn* ^{ts2} and *stn* ^{c} were uncovered by *Df(1)HM430, stn* $^{13–120}$, and *stn* ^{PH1} and were complemented by *y* $^{+}$*Ymal* $^{+}$. All phenotypes we observed were recessive: EJPs and mejps in *stn* ^{ts2}/+, *stn* ^{c}/+ *Df(1)HM430*/+, *stn* $^{13–120}$/+, *stn* ^{PH1}/+, and +/*y* $^{+}$*Ymal* $^{+}$ were similar to wild-type. Thus, all *stn* ^{ts2} and *stn* ^{c} phenotypes map to the *stoned* locus (Table 1).

Interestingly, *stn* ^{ts2} fails to complement fully the reduced EJP phenotype of *stn* ^{c} although *stn* ^{ts2} homozygotes do not show detectable reductions in EJP amplitude. This observation further suggests that *stn* ^{ts2}, in terms of the EJP phenotype, is a weak, partially expressive allele of *stoned* (Table 1). Overall, our complementation studies show that the synaptic transmission defects of *stn* ^{ts2} and *stn* ^{c} map specifically to the *stoned* locus. The recessive nature of the phenotypes suggests that the synaptic defects derive from a loss of function or expression of stonedA.

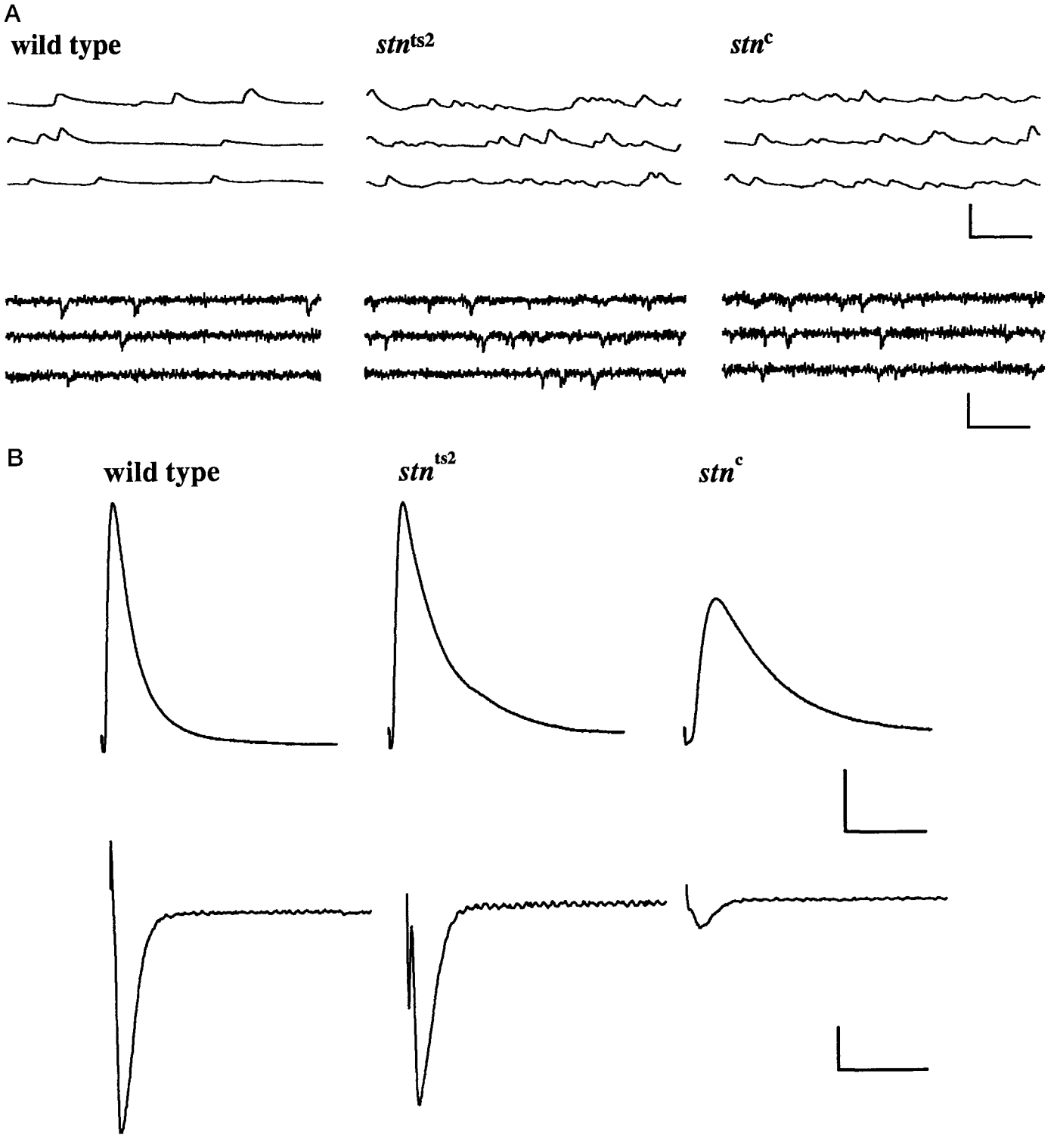

Figure 2. The *stn*^{ts2} and *stn*^{c} mutations affect both spontaneous and evoked synaptic activity at the larval NMJ. *A*, Three consecutive sweeps show representative mejps (*top traces*) and mejcs (*bottom traces*) recorded from wild-type, *stn*^{ts2}, and *stn*^{c} NMJs at 1.5 mM Ca^{2+}. mejcs were low-pass-filtered at 1 kHz. Calibration: 4 mV, 200 msec for mejps; 2 nA, 100 msec for mejcs. *B*, Representative EJPs (*top traces*) and EJCs (*bottom traces*) recorded from wild-type, *stn*^{ts2}, and *stn*^{c} NMJs at 1.5 mM Ca^{2+}. EJCs were low-pass-filtered at 1 kHz. Calibration: 10 mV, 50 msec for EJPs; 25 nA, 25 msec for EJCs.

Table 1. Enhanced mini frequency (mejps/sec) of stn^{ts2} and stn^{c} mutants maps to the *stoned* locus

	/+	/stn^{ts2}	/stn^{c}	/$y^{+}Ymal^{+}$	/$stn^{13\text{-}120}$	/stn^{PH1}	/*Df(1)HM430*
+/	4.8 ± 0.4 (24)	5.0 ± 0.8 (11)	7.0 ± 1.4 (10)	4.8 ± 0.6 (4)	4.6 ± 0.6 (5)	6.0 ± 0.4 (4)	6.0 ± 1.1 (5)
stn^{ts2}/		14.1 ± 0.6 (17)	11.2 ± 0.8 (9)	6.8 ± 0.7 (7)	10.7 ± 1.0 (8)	11.0 ± 1.2 (8)	15.8 ± 0.8 (7)
stn^{c}/			14.2 ± 0.8 (11)	4.5 ± 0.8 (10)	11.2 ± 0.9 (9)	17.0 ± 0.7 (7)	14.2 ± 0.7 (5)

Table 2. Reduced EJP amplitude (mV) of stn^{c} mutants maps to the *stoned* locus

	/+	/stn^{ts2}	/stn^{c}	/$y^{+}Ymal^{+}$	/$stn^{13\text{-}120}$	/stn^{PH1}	/*Df(1)HM430*
+/	39.2 ± 2.4 (22)	33.3 ± 1.8 (11)	47.7 ± 3.1 (8)	39.8 ± 4.0 (4)	35.1 ± 5.2 (5)	54.1 ± 1.9 (4)	45.3 ± 3.6 (5)
stn^{ts2}/		41.2 ± 2.1 (14)	31.7 ± 1.4 (12)	39.2 ± 3.8 (8)	35.4 ± 1.7 (7)	35.2 ± 1.6 (8)	36.8 ± 2.6 (7)
stn^{c}/			20.1 ± 2.4 (11)	37.6 ± 1.1 (8)	23.4 ± 3.2 (9)	17.6 ± 3.6 (7)	23.8 ± 2.7 (5)

Enhanced transmission variability, increased transmission failure, and decreased quantal content indicate that stn^{c} impairs evoked neurotransmitter release

Although the enhanced mini frequencies of stn^{ts2} and stn^{c} point to a presynaptic function for stonedA, the decrement in evoked response at stn^{c} NMJs theoretically could be a consequence of either presynaptic or postsynaptic defects. We found that EJP amplitudes were twice as variable in individual stn^{c} larvae as compared with individual wild-type larvae ($p = 0.002$) (Fig. 3*A*). Because the number of neurotransmitter receptors and ion channels on postsynaptic membrane should not show stochastic variation, the enhanced EJP variability most likely reflects variability in the number of neurotransmitter quanta released on stimulation of stn^{c} motor terminals. This suggests that stn^{c} mutants do not suffer a simple block in postsynaptic responsiveness to neurotransmitter. The enhanced EJP variability of stn^{c} mutants was not complemented by $y^{+}Ymal^{+}$. Nonetheless, EJP variability was low in stn^{c}/+ heterozygotes and was exacerbated by $stn^{13\text{–}120}$, stn^{PH1}, and *Df(1)HM430* (Fig. 3*A*). Thus, loss of stonedA function may reduce the tight coupling between neurotransmitter release and voltage-dependent Ca^{2+} entry at nerve terminals.

Further evidence for defects in evoked neurotransmitter release at stn^{c} NMJs is provided by failure–frequency analysis (Fig. 3*B*). We reduced extracellular Ca^{2+} to 0.3 mM, a level at which quantal variation in EJPs can be observed in wild-type. We then compared how often synaptic transmission failed at stn^{c} and control NMJs subjected to repetitive stimulation. Under these conditions, nerve stimulation failed to evoke a postsynaptic response nearly 50% of the time at stn^{c} NMJs, whereas failure occurred only 16% of the time at wild-type NMJs ($p = 0.003$) (Fig. 3*B*). The failure frequency of $stn^{c}/stn^{13\text{–}120}$ NMJs was not significantly different from that of stn^{c} NMJs, and the failure frequency of $stn^{c}/y^{+}Ymal^{+}$ NMJs was not significantly different from that of wild-type NMJs (Fig. 3*B*). The enhanced rate of transmission failure at stn^{c} NMJs under low Ca^{2+} conditions strongly suggests an impairment of Ca^{2+}-dependent neurotransmitter release from stn^{c} presynaptic terminals.

To assess the magnitude to which Ca^{2+}-dependent neurotransmitter release is impaired in stn^{c} mutants, we determined quantal content, a direct estimate of the number of synaptic vesicles fusing during a single evoked event. Because EJCs and mejcs represent linear responses of the muscle to neurotransmitter, we calculated mean quantal content (m) for wild-type and stn^{c} from the mean peak amplitudes of EJCs and mejcs (m = EJC/mejc) at 1.5 mM Ca^{2+}. Mean quantal content at stn^{c} NMJs ($m = 26.6 \pm 5.6$) was fivefold smaller than that at wild-type NMJs ($m = 127.8 \pm 11.2$; $p = 2.2 \times 10^{-5}$) (Fig. 3*C*). An interesting observation is that, when compared with wild-type mejcs (1.0 ± 0.07 nA), stn^{ts2} mejcs (0.8 ± 0.05 nA; $p = 0.03$) and stn^{c} mejcs (0.6 ± 0.03 nA; $p = 5 \times 10^{-4}$) were consistently smaller in amplitude. The reduced quantal size in stn^{ts2} and stn^{c} mutants raises the possibility that muscle-derived stonedA, the presence of which is hinted at by immunocytochemistry (see Fig. 1), in some way regulates postsynaptic sensitivity to neurotransmitter. It is equally plausible that alterations in presynaptic stonedA affect either the amount of neurotransmitter packaged within synaptic vesicles or change postsynaptic responsiveness via a homeostatic mechanism. Although further experiments are required to investigate these possibilities, reduced quantal content at stn^{c} NMJs unequivocally indicates that mutations of stonedA affect neurotransmitter release.

We next sought to determine whether this reduction in Ca^{2+}-dependent neurotransmitter release at stn^{c} NMJs represents a static uncoupling of neurotransmitter release from presynaptic Ca^{2+} entry or a change in the dynamic Ca^{2+} sensitivity of the release machinery, as observed in some *synaptotagmin* mutants (Littleton et al., 1993). An estimate of Ca^{2+} sensitivity can be obtained from the slope of a log–log plot of extracellular Ca^{2+} concentration versus peak EJC amplitude. We thus recorded EJCs at 0.3, 0.5, and 0.7 mM extracellular Ca^{2+}, a concentration range unlikely to saturate the release machinery (Fig. 4). We found that the log–log relationships between extracellular $[Ca^{2+}]$ and EJC amplitude were comparable for wild-type, stn^{c}, and stn^{ts2} (Fig. 4). Thus, although Ca^{2+}-dependent neurotransmitter release is impaired at stn^{c} NMJs, the sensitivity of neurotransmitter release to relative Ca^{2+} levels is unaltered.

Subtle alterations in presynaptic morphology cannot explain the physiological phenotypes of *stoned* mutants

The electrophysiological phenotypes of stn^{ts2} and stn^{c} mutants demonstrate that stonedA is required for normal levels of spontaneous and evoked synaptic activity at the third instar larval NMJ. To exclude the possibility that these phenotypes arise from gross disorganization of synapses, we examined *stoned* nerve terminals by EM. We examined general synapse ultrastructure and quantified the number, density, and size of synaptic vesicles in wild-type, stn^{ts2}, and stn^{c} boutons (Fig. 5*A–C*). The fractional area occupied by vesicles was not significantly different among

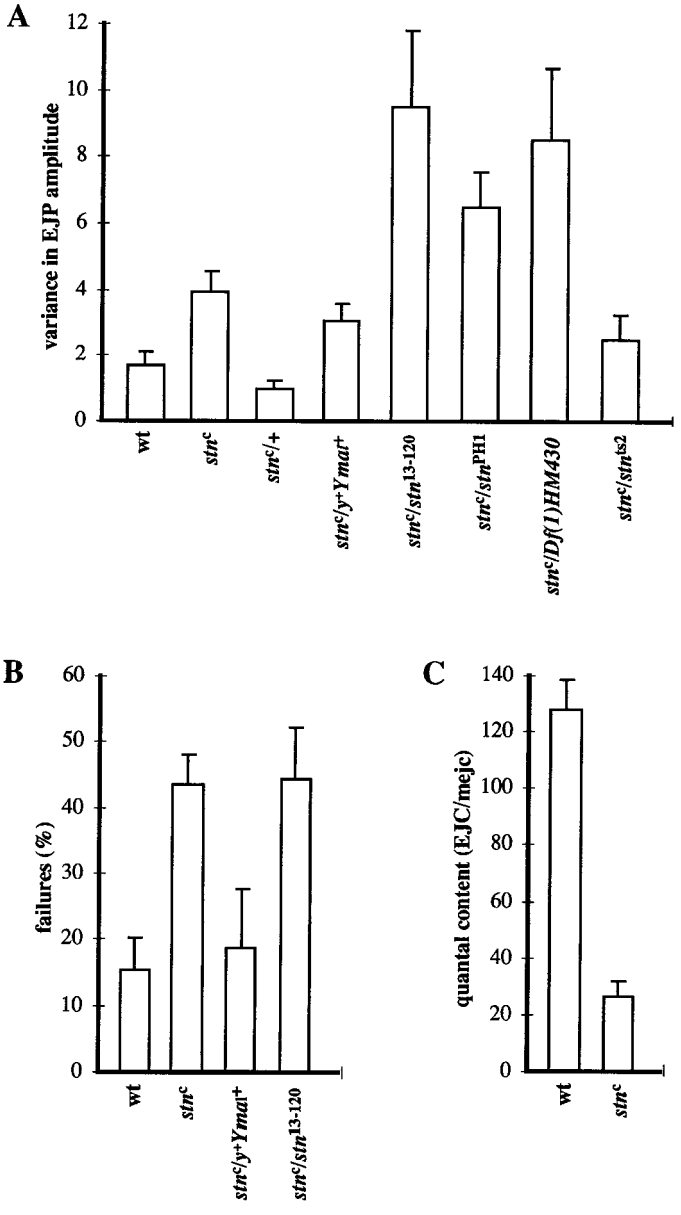

Figure 3. The *stn*^{c} mutation impairs evoked neurotransmitter release. *A*, *stn*^{c} mutants exhibit enhanced variability in EJP amplitude during trials of 1 Hz stimulation at 1.5 mM Ca^{2+}. The variance in EJP amplitude at individual NMJs was determined from measurements of 25–50 consecutive EJPs. The graph depicts mean EJP variances and SEMs. For the numbers of larvae examined from each genotype, refer to Table 1. *B*, *stn*^{c} mutants exhibit an increased frequency of synaptic transmission failures. To enhance the occurrence of failures at wild-type and *stn*^{c} NMJs, we reduced extracellular Ca^{2+} to 0.3 mM. The graph shows the mean ± SEM numbers of failures occurring from 100 stimuli delivered at 1 Hz; $n = 5$–7 larvae for each genotype. *C*, *stn*^{c} mutants exhibit a reduction in quantal content. EJCs and mejcs were recorded in 1.5 mM Ca^{2+} by clamping muscle 6 at −70 mV. Ten EJCs, elicited by 1 Hz stimulation, were averaged for each NMJ. Because mejc size was considerably more variable, 30–100 mejcs were averaged for each NMJ. The *open bars* depict mean quantal content ± SEM, which was calculated from mean EJC amplitude divided by mean mejc amplitude; $n = 7$ larvae for each genotype.

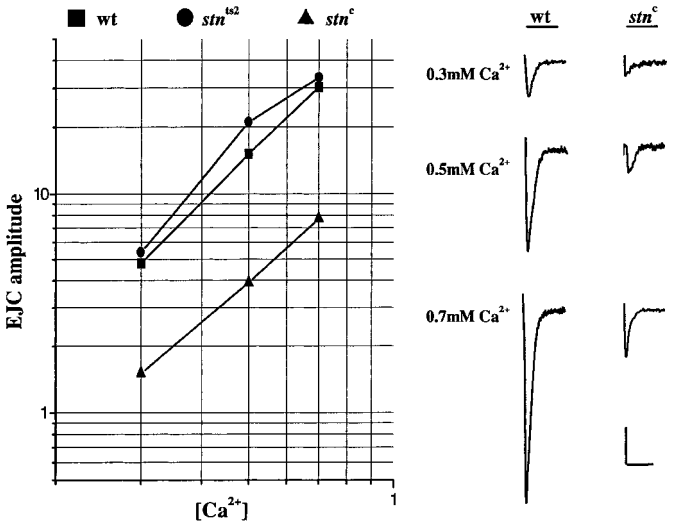

Figure 4. Neurotransmitter release maintains wild-type sensitivity to relative levels of extracellular Ca^{2+} in *stn*^{c} mutants. Each *point* on the log–log plot represents average EJC amplitudes from three to nine larvae. Representative EJCs at three subphysiological Ca^{2+} concentrations are shown for wild-type (*wt*) and *stn*^{c} NMJs. Calibration: 5 nA, 25 msec.

wild-type, *stn*^{ts2}, and *stn*^{c} boutons, although there was a trend toward wider synaptic vesicle distribution within *stn*^{ts2} and *stn*^{c} boutons (Fig. 5*D*). We found that wild-type and *stn*^{ts2} boutons had approximately equivalent synaptic vesicle densities, whereas *stn*^{c} boutons had a small but significant increase in synaptic vesicle density ($p = 0.009$) (Fig. 5*D*). Synaptic vesicles themselves were indistinguishable between wild-type (diameter, 34.0 ± 0.47 nm) and *stoned* mutants (32.8 ± 0.51 nm in *stn*^{ts2}; 34.2 ± 0.51 nm in *stn*^{c}). Thus, we observed no major ultrastructural changes in *stoned* mutant motor terminals; specifically, there was no depletion of morphologically defined synaptic vesicles and no gross abnormalities that could form the basis for the electrophysiological defects of *stoned* mutants.

We further counted the number of synaptic contact sites (boutons) over larval muscles 6 and 7. An increased number of synaptic sites could, in principle, produce the enhanced mini frequencies of *stoned* mutants; likewise, a decreased number of synaptic sites could give rise to the small evoked response of *stn*^{c} mutants. To gain insight into potential origins of these phenotypes, we used an antibody to synaptotagmin to visualize and examine neuromuscular synapses of wild-type, *stn*^{ts2}, and *stn*^{c} NMJs (Fig. 6*A–C*). We found that the number of boutons per arbor was slightly, but significantly, increased at both *stn*^{ts2} and *stn*^{c} NMJs (83.3 ± 4.6, $p = 0.04$; 96.2 ± 3.5, $p = 9.8 \times 10^{-6}$) as compared with wild-type (70.6 ± 3.8) (Fig. 6*D*). Although these differences raise interesting questions, the increase in bouton number cannot explain the decrease in evoked synaptic transmission at *stn*^{c} NMJs. Furthermore, these differences represent only 18 and 36% increases in bouton number at *stn*^{ts2} and *stn*^{c} NMJs, respectively, and cannot account for the ~300% increase in mini frequency at *stn*^{ts2} and *stn*^{c} NMJs. Thus, the physiological phenotypes of *stn*^{ts2} and *stn*^{c} mutants most likely arise from defective regulation of synaptic vesicle fusion within individual boutons.

Unexpectedly, during our light microscopic analyses of *stn*^{ts2} and *stn*^{c} NMJs we observed distinct alterations in the presynaptic localization of the synaptic vesicle proteins synaptotagmin and cysteine string protein (csp) at *stn*^{c} terminals. These alterations were difficult to quantify, but in "blind" tests we were able to distinguish between wild-type and *stn*^{c} preparations stained with anti-synaptotagmin (or anti-csp) antibodies with close to 100% accuracy. As shown previously (Estes et al., 1996), the distribu-

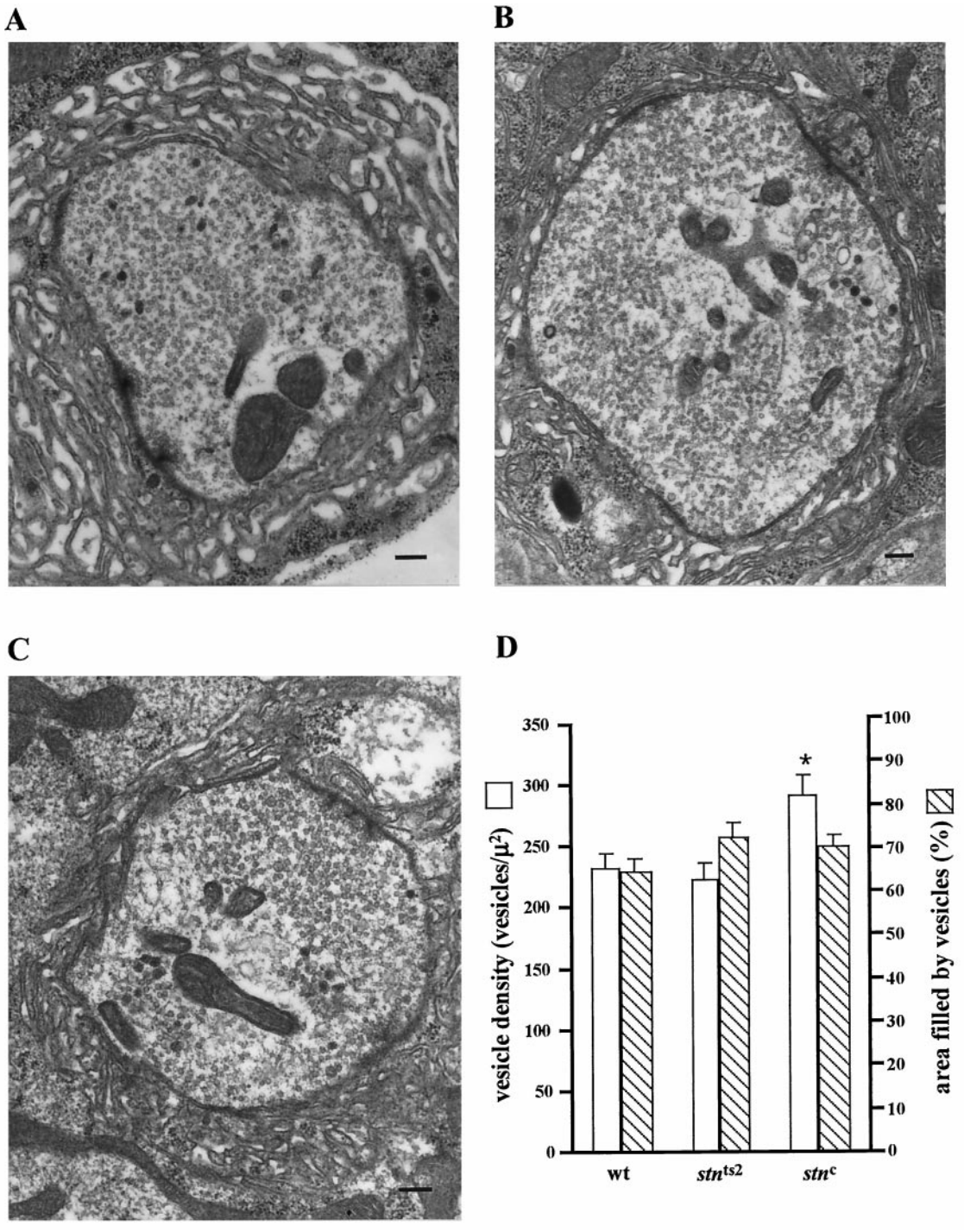

Figure 5. Normal ultrastructure of *stoned* mutant nerve terminals. Representative electron micrographs of type I presynaptic terminals on muscles 6 and 7 of third instar larvae are shown: wild-type (*A*); stn^{ts2} (*B*); stn^{c} (*C*). Scale bar, 200 nm. The graph shows mean synaptic vesicle content as determined by two independent measures. *Open bars* depict the mean number of synaptic vesicles per μm^2 within a bouton ± SEM. *Hatched bars* depict how much of a bouton (mean percentage area ± SEM) is filled by synaptic vesicles; areas that exclude synaptic vesicles are occupied by microtubules, mitochondria, or other subcellular structures. The size of synaptic vesicles in *stoned* mutant boutons (diameter, 32.8 ± 0.51 nm in stn^{ts2} and 34.2 ± 0.51 nm in stn^{c}) was not significantly different from wild-type boutons (34.0 ± 0.47 nm). Analyses of other synaptic features, including the folding of the subsynaptic reticulum, revealed no systematic differences between *stoned* and wild-type preparations. $n = 28$ for wild-type, 30 for stn^{ts2}, and 28 for stn^{c} boutons.

tion of synaptotagmin and csp within wild-type presynaptic boutons reflects the expected locations of synaptic vesicle pools—synaptotagmin and csp both are highly concentrated within boutons but are excluded from intervening axonal regions (Fig. 6*E*) (data not shown). There also are small regions within boutons that are devoid of synaptotagmin and csp.

In general, stn^{c} mutants appeared to show an increase in synaptotagmin and csp immunoreactivity at the bouton periphery (Fig. 6*G*). In addition, we frequently observed synaptotagmin and csp immunoreactivity in axonal regions connecting boutons (Fig. 6*G*). Alterations in stn^{ts2} boutons were more subtle, and some stn^{ts2} preparations were not easily distin-

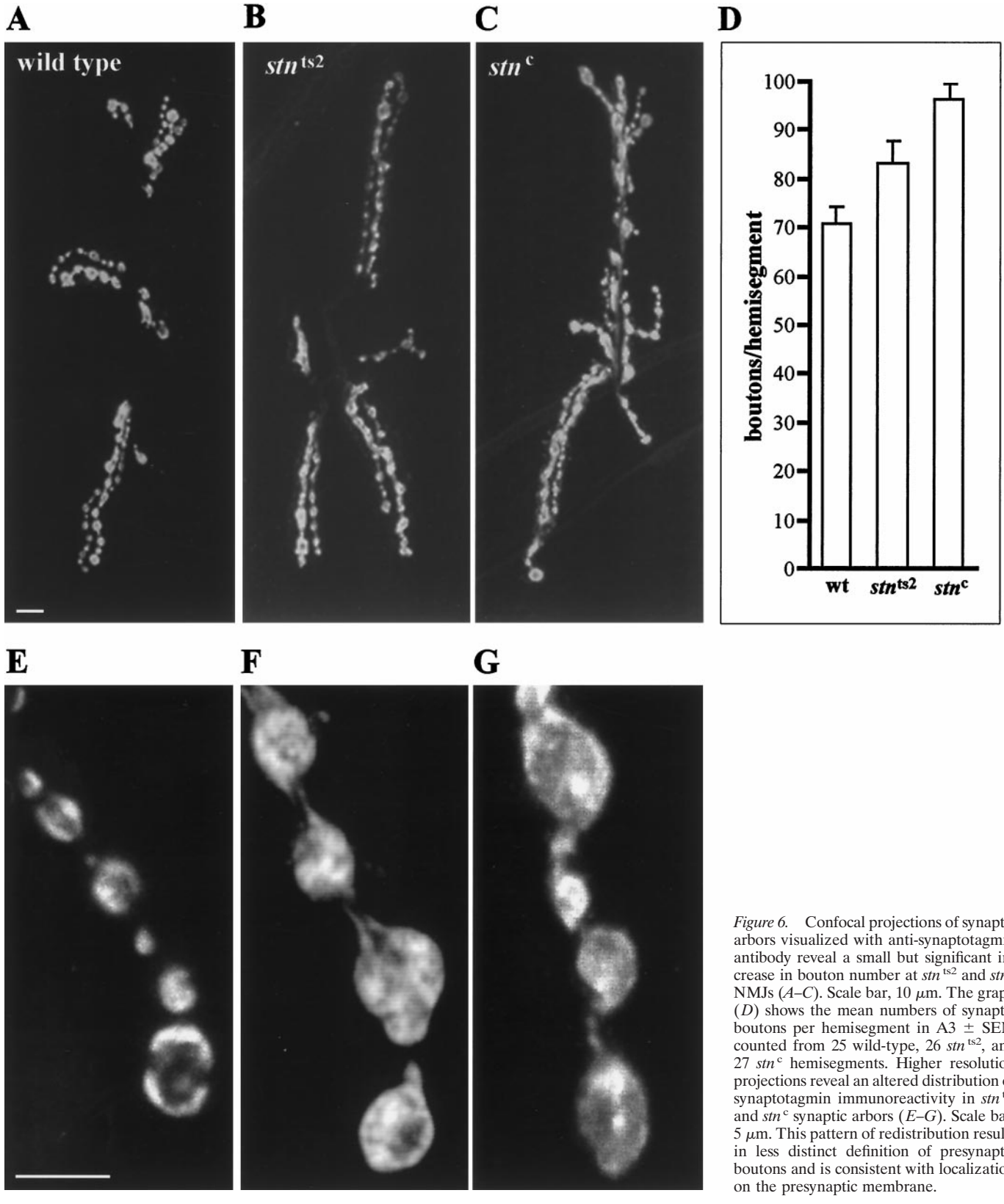

Figure 6. Confocal projections of synaptic arbors visualized with anti-synaptotagmin antibody reveal a small but significant increase in bouton number at *stn* ^{ts2} and *stn* ^{c} NMJs (*A–C*). Scale bar, 10 μm. The graph (*D*) shows the mean numbers of synaptic boutons per hemisegment in A3 $\pm$ SEM counted from 25 wild-type, 26 *stn* ^{ts2}, and 27 *stn* ^{c} hemisegments. Higher resolution projections reveal an altered distribution of synaptotagmin immunoreactivity in *stn* ^{ts2} and *stn* ^{c} synaptic arbors (*E–G*). Scale bar, 5 μm. This pattern of redistribution results in less distinct definition of presynaptic boutons and is consistent with localization on the presynaptic membrane.

guishable from wild-type (Fig. 6*F*). These altered patterns of synaptotagmin and csp immunoreactivity in *stoned* boutons could suggest that synaptotagmin and csp are not recycled efficiently from the plasma membrane and consequently diffuse laterally through the membrane. However, no synaptic vesicle depletion or major morphological alterations are apparent in *stn* ^{c} nerve terminals viewed under the electron microscope. Possible interpretations of the morphological alterations we

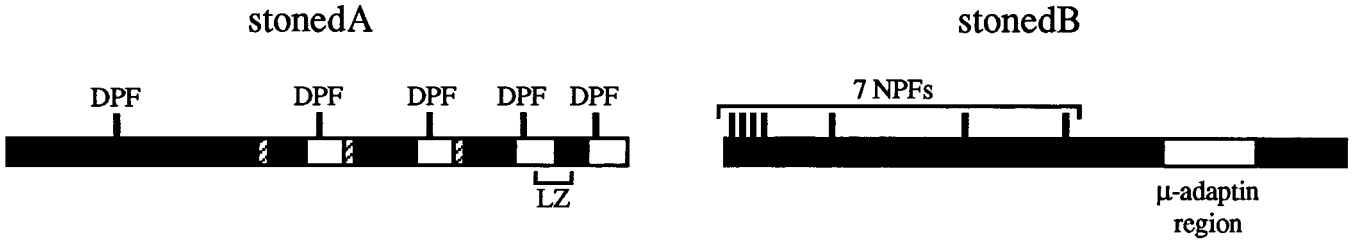

Figure 7. Domain structures of stonedA and stonedB. StonedA contains four novel "long" (28–55 amino acids) repeats (*open rectangles*); the C-terminal-most pair of these are truncations of the N-terminal-most pair. Three octomeric repeats enriched in acidic amino acids (*hatched areas*) overlap with the long repeats. DPF repeats (*vertical bars*), which are contained in a region of Eps15 shown to bind α-adaptin, are enriched in the long repeats, but one also is present near the N terminus. A leucine zipper (*LZ*) overlaps with the third long repeat. StonedB contains seven NPF motifs (*vertical bars*), which constitute recognition sites for the EH domain of Eps15 and related proteins. The C terminus of stonedB contains a ~250 amino acid sequence with 42% identity to the μ-adaptin family of proteins (*open rectangle*).

observe under the light microscope are considered in Discussion.

DISCUSSION

The *stoned* gene first was associated with nervous system function when the mutants stn^{ts2} and stn^{c} were isolated on the basis of obvious behavioral abnormalities (Grigliatti et al., 1973; Homyk, 1977; Homyk and Sheppard, 1977). Subsequent genetic and phenotypic studies provided indirect evidence that *stoned* gene products might be required for synaptic transmission (Petrovich et al., 1993; Andrews et al., 1996). In this paper we demonstrate that a product of the *stoned* gene is present at presynaptic terminals and is involved in the regulation of neurotransmitter release. Thus, our analysis provides the first direct evidence that a *stoned* gene product regulates presynaptic functions.

Genetic and phenotypic analysis of *stoned*

The *Drosophila stoned* locus is extremely unusual in its organization: a single dicistronic transcript from the gene encodes two structurally unrelated polypeptides termed stonedA and stonedB (Andrews et al., 1996) (Fig. 7). Thus, unlike most genetic loci, single mutational events could cause phenotypes that result from defects in both molecules. This is likely the case for the lethal alleles of *stoned* used in this study (Andrews et al., 1996). However, the viable alleles of *stoned*, stn^{ts2} and stn^{c}, recently have been shown to carry missense mutations that alter the stonedA product (A. M. Phillips and M. Smith, unpublished observations). Although complex effects of these single base substitutions on transcript stability or on translation rates of the second cistron cannot be excluded completely, it is likely that these missense mutations affect activity of only the stonedA protein. StonedA is enriched at nerve terminals where its levels are reduced substantially in stn^{c} mutants (see Fig. 1). Thus, it is likely that the neurological phenotypes of stn^{ts2} and stn^{c} mutants result from altered stonedA function.

Our analyses of stn^{ts2} and stn^{c} mutants and other allelic combinations that survive to the third larval instar show that several properties of neurotransmitter release are altered by a disruption of stonedA. Mutant stn^{c} and stn^{ts2} larvae exhibit similar rates of spontaneous neurotransmitter release that are elevated approximately threefold over wild-type (see Fig. 2*A*, Table 1). The quantal content of the evoked response is reduced significantly in stn^{c} mutants (see Fig. 3*C*), a phenotype that is not complemented by stn^{ts2}, although stn^{ts2} homozygotes do not themselves show perceptible defects in evoked transmitter release (see Fig. 2*B*, Table 2). In addition to reduced quantal content, stn^{c} mutations cause reduced fidelity in neurotransmission (see Fig. 3*A,B*). All phenotypes of stn^{c} or stn^{ts2} homozygotes described above are uncovered by deficiencies or lethal alleles of *stoned* and complemented by a small chromosomal duplication that includes the *stoned* locus (Tables 1, 2); thus, these defects are caused by mutations in *stoned*.

Although stonedA may have additional, as yet unknown, functions in other tissues, our electrophysiological studies suggest that an important function of stonedA is to regulate the presynaptic release of neurotransmitter. However, these studies alone do not exclude the possibility that functional defects in *stoned* mutants arise from a primary defect in, for instance, synapse development or organization. To address this issue, we examined *stoned* synapses by EM. Our analysis did not reveal any ultrastructural defects that could account for the physiological defects we observed at *stoned* synapses. Thus, the data suggest that altered regulation of synaptic vesicle fusion is the primary defect in *stoned* mutants. An alternative that we have not excluded in our studies is that a subset of synaptic vesicle membrane proteins, required for function but not for assembly of synaptic vesicles, is not recycled correctly in *stoned* mutants. In this scenario the altered regulation of transmitter release that is observed in *stoned* mutants could arise from a primary defect in an unprecedented, novel pathway for the recycling of specific membrane component(s) of synaptic vesicles. Below, we discuss and try to reconcile these two alternative roles that stonedA may play in synaptic vesicle cycling.

StonedA as part of the Ca^{2+}-sensitive fusion clamp

The elevated rate of spontaneous neurotransmitter release from stn^{ts2} and stn^{c} motor terminals suggests that in wild-type synapses stonedA function limits the rate of Ca^{2+}-independent synaptic vesicle fusions. Furthermore, the reduction in evoked neurotransmitter release from stn^{c} motor terminals suggests that stonedA normally promotes Ca^{2+}-dependent synaptic vesicle fusions. Such a dual role in regulating synaptic vesicle exocytosis has been postulated previously for synaptotagmin, a synaptic vesicle membrane protein with two calcium-binding C_2 domains (Popov and Poo, 1993). Mutations of synaptotagmin in *Drosophila* give rise to phenotypes strikingly similar to those of *stoned* mutants (Littleton et al., 1993, 1994; DiAntonio and Schwarz, 1994). Like stn^{c} mutants, *Drosophila synaptotagmin* (*syt*) mutants exhibit an approximately threefold enhanced rate of spontaneous neurotransmitter release and a severe reduction in evoked neurotransmitter release. These observations led to the proposal that synaptotagmin acts as a Ca^{2+}-sensitive fusion clamp that inhibits synaptic vesicle fusion in the absence of Ca^{2+} but facilitates synaptic vesicle fusion in response to presynaptic Ca^{2+} entry. Such a role for synaptotagmin is supported by a number of biochemical studies (for review, see Sudhof and Rizo, 1996; Bennett, 1997).

The biochemical properties of stonedA are not as well characterized as those of synaptotagmin, and so the detailed mechanisms by which it may regulate transmitter release remain to be discovered. Unlike the case for synaptotagmin, there is no evidence that stonedA is capable of sensing and responding to cytosolic Ca^{2+} levels. First, although stonedA contains clusters of acidic residues (see Fig. 7), it does not contain C_2 domains or any other consensus Ca^{2+}-binding domains. Second, although synaptic vesicle fusion in *stn*^{c} mutants is uncoupled partially from Ca^{2+}, evoked neurotransmitter release in the mutant remains sensitive to Ca^{2+} (see Fig. 4). A recent observation that recombinant stonedA can bind to recombinant synaptotagmin *in vitro* (A. M. Phillips, unpublished results) opens the possibility that stonedA interacts with synaptotagmin to regulate synaptic vesicle fusion in a Ca^{2+}-dependent manner.

A possible role for stonedA in synaptic vesicle recycling

Genetic interactions between *stn*^{ts2} and *shi*^{ts1} led to the suggestion that a *stoned* product might regulate synaptic vesicle recycling (Petrovich et al., 1993). Our recent analysis of the stonedA sequence shows that its C-terminal region contains four DPF repeats (see Fig. 7), which define a C-terminal domain of Eps15, a protein believed to be involved in membrane internalization (Benmerah et al., 1996). A functional role for the DPF motif is suggested by a recent study that demonstrates that the binding of human Eps15 to the α-adaptin subunit of AP-2 is mediated by a portion of Eps15 that contains four of these DPF repeats (Benmerah et al., 1996). It may be significant that stonedB contains Eps15-binding domains that potentially could interact with the Eps15-like sequences of stonedA.

When we screened protein databases for other polypeptides with DPF repeats, we discovered a rather selective enrichment of two or more closely spaced DPFs in several presynaptic proteins, including Eps15, the clathrin-uncoating cofactor auxilin (Ungewickell et al., 1995) (Entrez accession number S68983; three DPFs), and the clathrin assembly protein AP180 (Ahle and Ungewickell, 1986) (accession number S36327; two DPFs). Other proteins containing DPF repeats are heat–shock proteins, the FMRFamide-related neuropeptides (accession numbers S38816, Q07981, P42565; 7–14 DPFs), phospholipase A-2-activating protein (accession numbers P27612, P54319; three DPFs), and phospholipase C (accession numbers A31225, P13217; two DPFs). Although we can only speculate about the function of DPF repeats in stonedA, the presence of multiple DPFs in Eps15, auxilin, and AP180 indicates a common structural feature among stonedA and proteins thought to be involved in clathrin-mediated endocytosis.

Despite the genetic interactions between *stn*^{ts2} and *shi*^{ts1}, and the sequence of stonedA, there is little direct evidence that *stoned* mutations affect synaptic vesicle recycling. Our EM data show that synaptic vesicles are not depleted in *stn*^{c} and *stn*^{ts2} nerve terminals, and these vesicles are not morphologically distinguishable from wild-type vesicles. However, as shown in Figure 6, under the fluorescence microscope we observe an altered distribution of the synaptic vesicle membrane proteins synaptotagmin and csp in *stn*^{c} mutants. This redistribution is consistent with an accumulation of synaptotagmin and csp throughout the presynaptic plasma membrane of *stn*^{ts2} and *stn*^{c} mutants (Estes et al., 1996). If synaptotagmin and csp are not retrieved efficiently from the plasma membrane in *stoned* boutons, it seems puzzling that *stoned* boutons show no alterations in synaptic vesicle number, distribution, or size. It is possible that a subset of synaptic vesicle proteins, including csp and synaptotagmin, recycle via a stonedA-dependent pathway, whereas others, required for the formation of morphologically identifiable synaptic vesicles, recycle in a stonedA-independent manner. If this were the case, then altered neurotransmitter release in *stoned* mutants may be a secondary consequence of ineffective synaptotagmin recycling into synaptic vesicles. A second, more conservative alternative is that the apparent redistribution of synaptotagmin and csp, although unequivocal under the fluorescence microscope, derive from a relatively minor fraction of synaptic vesicle proteins that are localized aberrantly. In this model, *stoned* mutants may have a minor defect in recycling of all synaptic vesicle membrane proteins; this defect is visible in our immunofluorescence studies but is so subtle as to be invisible under the electron microscope. Although additional experiments are required to assess the endocytosis of different synaptic vesicle membrane proteins in *stn*^{ts2} and *stn*^{c} mutants, our working hypothesis is that stonedA regulates both synaptic vesicle fusion and endocytosis.

StonedA is not the first protein for which dual roles in synaptic vesicle exocytosis and endocytosis have been proposed. Both biochemical and genetic studies suggest that, in addition to its role in regulating synaptic vesicle fusion, synaptotagmin may regulate synaptic vesicle recycling (Zhang et al., 1994; Jorgensen et al., 1995; Sudhof and Rizo, 1996). Although the possible role of synaptotagmin in synaptic vesicle recycling has not been addressed in studies of *Drosophila syt* mutants, *Caenorhabditis elegans synaptotagmin* (*snt-1*) mutants exhibit phenotypes consistent with impaired synaptic vesicle recycling (Jorgensen et al., 1995). For example, the synaptic vesicle protein synaptobrevin exhibits an abnormally diffuse distribution in the *snt-1* nerve cord, suggesting an accumulation and lateral spreading of this protein within neuronal plasma membrane (Jorgensen et al., 1995). This altered distribution of synaptobrevin in *snt-1* nerve cord is qualitatively similar to the altered distributions of synaptotagmin and csp in *stoned* boutons. Thus, parallels between *stoned* mutants and *synaptotagmin* mutants suggest that stonedA and synaptotagmin may share functions in synaptic vesicle recycling as well as in synaptic vesicle fusion.

If stonedA does in fact regulate general synaptic vesicle endocytosis, could defects in transmitter release at *stn*^{ts2} and *stn*^{c} synapses be secondary to a primary defect in synaptic vesicle recycling? We believe this to be unlikely for the following reasons. First, our EM studies show that any recycling defects at *stn*^{ts2} and *stn*^{c} mutant synapses must be very subtle. Second, partial depletion of synaptic vesicles, which may be achieved by stimulating *shi*^{ts1} mutants at nonpermissive temperature, does not result in the specific phenotypes we observe at *stoned* mutant synapses (Koenig et al., 1983). The elevated mini frequency and the reduced evoked release are unique phenotypes of *stoned* mutants and thus probably reflect a specific function of stonedA in regulating Ca^{2+}-dependent neurotransmitter release. The simplest interpretation of our data is that *stn*^{ts2} and *stn*^{c} mutants have independent defects in synaptic vesicle fusion and synaptic vesicle recycling.

Other possible functions of stonedA

In addition to regulating basal presynaptic functions, stonedA may be involved in a cAMP-dependent pathway that regulates synapse plasticity. Genetic studies have shown synthetic lethality between *stn*^{ts2} and *dnc*^{M14}, a mutation that affects a cAMP phosphodiesterase (Petrovich et al., 1993). The *dunce* gene product has been implicated in learning and memory and appears to be an important component of cAMP-responsive pathways that

regulate gene expression as well as structural and functional remodeling of synapses (Davis, 1996). It is interesting that *stn*^{ts2} and *stn*^{c} mutants cause small but significant increases in bouton number at the larval NMJ, a phenotype that has been described for *dnc*^{M14} (Zhong et al., 1992; Schuster et al., 1996). This somewhat tenuous association between a mutation in the cAMP pathway and *stoned* could indicate that stonedA participates in the regulation of synapse plasticity and perhaps plays some role in learning and memory (Petrovich et al., 1993).

Identification of other gene products that interact with stonedA, either directly or indirectly, will facilitate further characterization of stonedA function. In addition, identification of stonedA homologs in other organisms will allow for the development of further tools to examine possible functions of stonedA. We have used a classical genetic approach to manipulate stonedA activity at a relatively simple, experimentally accessible synapse in *Drosophila*. Our results establish that stonedA is an influential regulator of synaptic vesicle exocytosis and suggest that stonedA may have additional functions in synaptic vesicle recycling and synaptic remodeling.

REFERENCES

Ahle S, Ungewickell E (1986) Purification and properties of a new clathrin assembly protein. EMBO J 5:3143–3149.

Andrews J, Smith M, Merakovsky J, Coulson M, Hannan F, Kelly LE (1996) The *stoned* locus of *Drosophila melanogaster* produces a dicistronic transcript and encodes two distinct polypeptides. Genetics 143:1699–1711.

Atwood HL, Govind CK, Wu C-F (1993) Differential ultrastructure of synaptic terminals on ventral longitudinal abdominal muscles in *Drosophila* larvae. J Neurobiol 24:1008–1024.

Benmerah A, Begue B, Dautry-Varsat A, Cerf-Bensussan N (1996) The ear of α-adaptin interacts with the COOH-terminal domain of the Eps15 protein. J Biol Chem 271:12111–12116.

Bennett MK (1997) Ca^{2+} and the regulation of neurotransmitter secretion. Curr Opin Neurobiol 7:316–322.

Condie JM, Brower DL (1989) Allelic interactions at the *engrailed* locus of *Drosophila*: engrailed protein expression in imaginal discs. Dev Biol 135:31–42.

Cremona O, De Camilli P (1997) Synaptic vesicle endocytosis. Curr Opin Neurobiol 7:323–330.

Davis RL (1996) Physiology and biochemistry of *Drosophila* learning mutants. Physiol Rev 76:299–317.

De Camilli P, Takei K (1996) Molecular mechanisms in synaptic vesicle endocytosis and recycling. Neuron 16:481–486.

DiAntonio A, Schwarz TL (1994) The effect on synaptic physiology of synaptotagmin mutations in *Drosophila*. Neuron 12:909–920.

DiAntonio A, Parfitt K, Schwarz TL (1993) Synaptic transmission persists in synaptotagmin mutants of *Drosophila*. Cell 73:1281–1290.

Estes PS, Roos J, van der Bliek A, Kelly RB, Krishnan KS, Ramaswami M (1996) Traffic of dynamin within individual *Drosophila* synaptic boutons relative to compartment-specific markers. J Neurosci 16:5443–5456.

Geppert M, Goda Y, Hammer RE, Li C, Rosahl TW, Stevens CF, Sudhof TC (1994) Synaptotagmin I: a major Ca^{2+} sensor for transmitter release at a central synapse. Cell 79:717–727.

Grant D, Unadkat S, Katzen A, Krishnan KS, Ramaswami M (1998) Probable mechanisms underlying intra-allelic complementation and temperature sensitivity of mutations at the *shibire* locus of *Drosophila melanogaster*. Genetics 149:1019–1030.

Grigliatti TA, Hall L, Rosenbluth R, Suzuki DT (1973) Temperature-sensitive mutations in *Drosophila melanogaster*. XIV. A selection of immobile adults. Mol Gen Genet 120:107–114.

Hanson PI, Heuser JE, Jahn R (1997) Neurotransmitter release—four years of SNARE complexes. Curr Opin Neurobiol 7:310–315.

Homyk Jr T (1977) Behavioral mutants of *Drosophila melanogaster*. II. Behavioral analysis and focus mapping. Genetics 87:105–128.

Homyk Jr T, Pye Q (1989) Some mutations affecting neural or muscular tissues alter the physiological components of the electroretinogram in *Drosophila*. J Neurogenet 5:37–48.

Homyk Jr T, Sheppard DE (1977) Behavioral mutants of *Drosophila melanogaster*. I. Isolation and mapping of mutations which decrease flight ability. Genetics 87:95–104.

Jan LY, Jan YN (1976) Properties of the larval neuromuscular junction in *Drosophila melanogaster*. J Physiol (Lond) 262:189–214.

Jorgensen EM, Hartwieg E, Schuske K, Nonet ML, Jin Y, Horvitz HR (1995) Defective recycling of synaptic vesicles in synaptotagmin mutants of *Caenorhabditis elegans*. Nature 378:196–199.

Katz B (1969) The Sherrington lectures, X. The release of neural transmitter substances. London: Liverpool UP.

Kelly LE (1983) An altered electroretinogram transient associated with an unusual jump response in a mutant of *Drosophila*. Cell Mol Neurobiol 3:143–149.

Kelly RB (1993) Storage and release of neurotransmitters. Cell 72:43–53.

Koenig JH, Saito K, Ikeda K (1983) Reversible control of synaptic transmission in a single gene mutant of *Drosophila melanogaster*. J Cell Biol 96:1517–1522.

Kosaka T, Ikeda K (1983) Possible temperature-dependent blockage of synaptic vesicle recycling induced by a single gene mutation in *Drosophila*. J Neurobiol 14:207–225.

Kurdyak P, Atwood HL, Stewart BA, Wu C-F (1994) Differential physiology and morphology of motor axons to ventral longitudinal muscles in larval *Drosophila*. J Comp Neurol 350:463–472.

Littleton JT, Stern M, Schulze K, Perin M, Bellen HJ (1993) Mutational analysis of *Drosophila synaptotagmin* demonstrates its essential role in Ca^{2+}-activated neurotransmitter release. Cell 74:1125–1134.

Littleton JT, Stern M, Perin M, Bellen HJ (1994) Calcium dependence of neurotransmitter release and rate of spontaneous synaptic vesicle fusions are altered in *Drosophila* synaptotagmin mutants. Proc Natl Acad Sci USA 91:10888–10892.

Matthews G (1996) Neurotransmitter release. Annu Rev Neurosci 19:219–233.

Petrovich TZ, Merakovsky J, Kelly LE (1993) A genetic analysis of the *stoned* locus and its interaction with *dunce*, *shibire*, and *suppressor* of *stoned* variants of *Drosophila melanogaster*. Genetics 133:955–965.

Popov SV, Poo MM (1993) Synaptotagmin: a calcium-sensitive inhibitor of exocytosis? Cell 73:1247–1249.

Robinson MS (1997) Coats and vesicle budding. Trends Cell Biol 7:99–102.

Salcini AE, Confalonieri S, Doria M, Santolini E, Tassi E, Minenkova O, Cesareni G, Pelicci PG, Di Fiore PP (1997) Binding specificity and *in vivo* targets of the EH domain, a novel protein–protein interaction module. Genes Dev 11:2239–2249.

Schuster CM, Davis GW, Fetter RD, Goodman CS (1996) Genetic dissection of structural and functional components of synaptic plasticity. II. Fasciclin II controls presynaptic structural plasticity. Neuron 17:655–667.

Stewart BA, Atwood HL, Renger JJ, Wang J, Wu C-F (1994) Improved stability of *Drosophila* larval neuromuscular preparations in haemolymph-like physiological solutions. J Comp Physiol [A] 175:179–191.

Sudhof TC (1995) The synaptic vesicle cycle: a cascade of protein–protein interactions. Nature 375:645–653.

Sudhof TC, Rizo J (1996) Synaptotagmins: C_2-domain proteins that regulate membrane traffic. Neuron 17:379–388.

Ungewickell E, Ungewickell H, Holstein SEH, Lindner R, Prasad K, Barouch W, Martin B, Greene LE, Eisenberg E (1995) Role of auxilin in uncoating clathrin-coated vesicles. Nature 378:632–635.

van der Bliek AM, Meyerowitz EM (1991) Dynamin-like protein encoded by the *Drosophila shibire* gene associated with vesicular traffic. Nature 351:411–414.

Warnock DE, Schmid SL (1996) Dynamin GTPase, a force-generating molecular switch. BioEssays 18:885–893.

Zhang JZ, Davletov BA, Sudhof TC, Anderson RGW (1994) Synaptotagmin I is a high affinity receptor for clathrin AP-2: implications for membrane recycling. Cell 78:751–760.

Zhong Y, Budnik V, Wu C-F (1992) Synaptic plasticity in *Drosophila* memory and hyperexcitable mutants: role of cAMP cascade. J Neurosci 12:644–651.

Zucker RS (1996) Exocytosis: a molecular and physiological perspective. Neuron 17:1049–1055.

Zusman S, Coulter D, Gergen JP (1985) Lethal mutations induced in the proximal X chromosome of *Drosophila melanogaster* using P-M hybrid dysgenesis. *Drosophila* Inform Serv 61:217–218.